Supporting Information

Influence of lithium and lanthanum treatment on TiO_2 nanofibers and their application in n-i-p solar cells

*Filip Ambroz[a], Sanjayan Sathasivam[a], Roxanna Lee[a], Srinivas Gadipelli[a], Chieh-Ting Lin[b,c], Shengda Xun[c], Radhika K. Poduval[d], Martyn Mclachlan[c], Ioannis Papakonstantinou[d], Ivan P. Parkin[a] and Thomas J. Macdonald[*a]*

[a] Department of Chemistry, University College London, 20 Gordon St, London, WC1H 0AJ, United Kingdom

[b] Department of Chemistry, Imperial College London, Imperial College Road, London, SW7 2AZ, United Kingdom

[c] Department of Materials and Centre for Plastic Electronics, Imperial College London, Imperial College Road, London, SW7 2AZ, United Kingdom

[d] Department of Electronic and Electrical Engineering, University College London, Torrington Place, London, WC1E 7JE, United Kingdom

[e] SPECIFIC IKC College of Engineering, Swansea University, Swansea, SA2 7AX, United Kingdom

Materials chemistry instrumentation details:

UV-Visible spectroscopy was performed with a Perkin Elmer Lambda 950 instrument with a measurement interval of 1 nm (Department of Chemistry, UCL). Transmission Electron Microscopy (TEM) was performed using a JEOL 2010 TEM operating at 200 kV (Department of Chemistry, UCL). Image collection and processing was performed on a CCD with Gatan Digital Micrograph software. Particle size analysis was carried out using ImageJ software. X-Ray diffraction (XRD) patterns were recorded using a Bruker D8 Discover X-ray diffractometer using monochromatic Cu $K_{\alpha 1}$ and Cu $K_{\alpha 2}$ radiation of wavelengths 1.54056 and 1.54439 Å respectively (Department of Chemistry, UCL). All XRD data was analysed using CrystalDiffract software and compared to the ICSD standard dataset. X-ray photoelectron spectroscopy (XPS) was carried out using a Thermo Scientific K-alpha photoelectron spectrometer with monochromatic Al-K_α radiation to analyze the Au nanostructures in TiO_2 photoelectrodes (Department of Chemistry, UCL). Peak positions were calibrated to carbon (285 eV) and plotted using the CasaXPS and qtiplot software.

Photovoltaic and Electrochemical characterization:

J–V measurements were performed under one-sun (AM 1.5G) illumination using a LOT calibrated solar simulator with a Xenon lamp. Devices were connected to a Keithley 2400 source meter to output the data. Photocurrent measurements were obtained with a halogen lamp chopped to a frequency of 188 Hz through a Newport monochromator; a 4-point probe in connection with a lock-in amplifier is used to collect data. The monochromatic beam is calibrated using a Silicon photo-diode. (Department of Electronic and Electrical Engineering, UCL Chemistry).

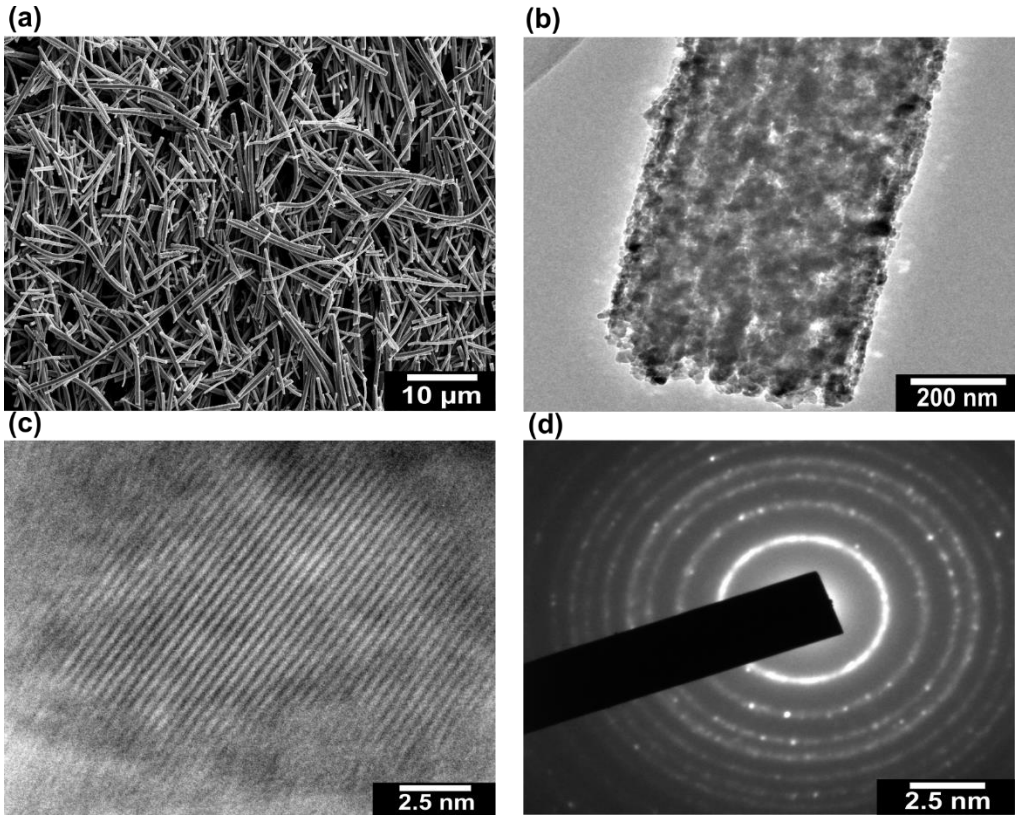

Figure S1. (a) Shows top-view SEM image of control TiO_2 NFs. (b) Shows a TEM image of a single isolated control TiO_2 nanofiber with lattice planes (c) confirming high crystallinity. (d) Shows SAED pattern of control TiO_2 NFs.

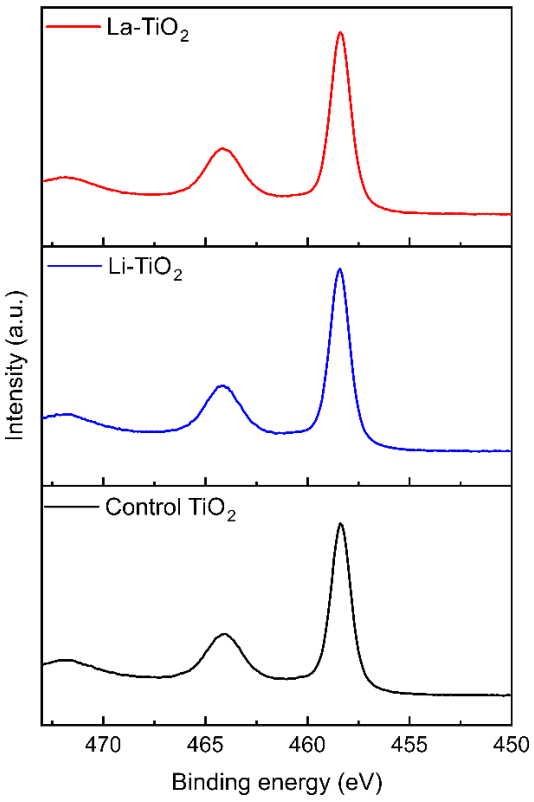

Figure S2. The Ti2p XPS spectrum for control, La-TiO_2 and Li-TiO_2 NFs.

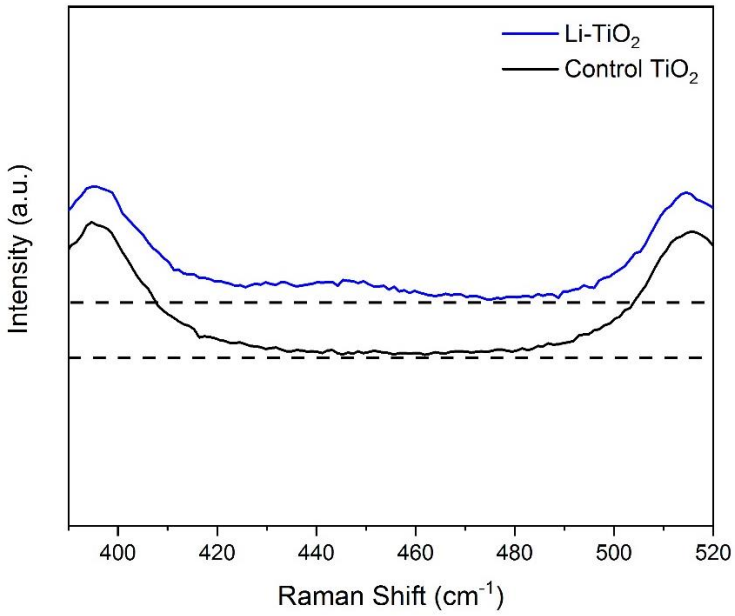

Figure S3. Inset of Raman surface scan for control and Li-TiO_2 NFs.

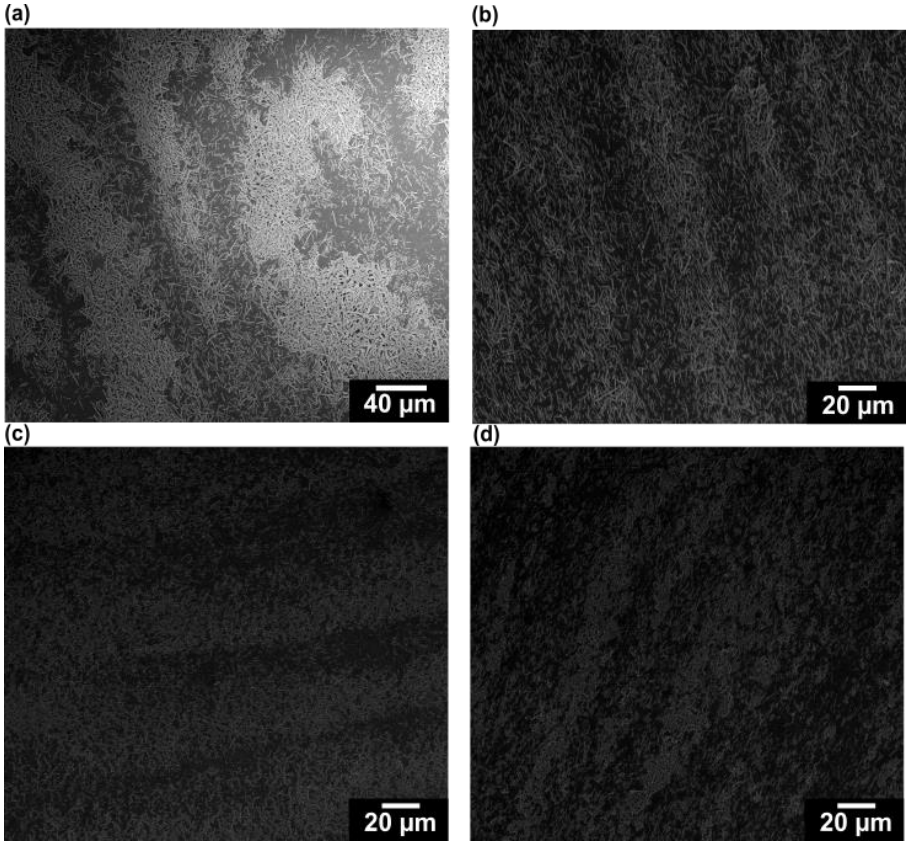

Figure S4. Top-view SEM image of control TiO_2 NFs for PSCs deposited for (a) 20 sec at 1000 RPM and 5 sec at 2000 RPM (60 mg/mL in ethanol, 4.9 g of terpineol per 1 g of NFs and 0.29 g of hydroxypropyl cellulose per 1 g of NFs), (b) 30 sec at 3000 RPM (30 mg/mL and 4.9 g of terpineol per 1 g of NFs), (c) 30 sec at 5000 RPM and (d) 30 sec at 6000 RPM.

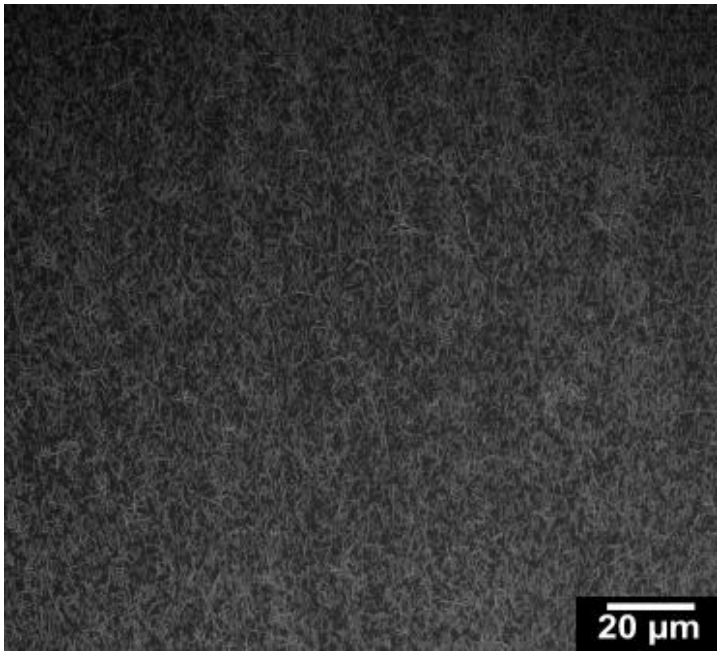

Figure S5. Top-view SEM image of control TiO_2 NFs for PSCs deposited at 4000 RPM for 30 sec.

Table S1. Lattice parameters and volumes for control, La-TiO_2 and Li-TiO_2 NFs.

	Lattice parameter a (Å)	**Lattice parameter c (Å)**	**Lattice volume (Å^3)**
Control TiO_2	3.78	9.49	135.60
La-TiO_2	3.80	9.46	136.33
Li-TiO_2	3.79	9.43	135.24

Table S2. The bandgap values obtained from the Tauc plots in Figure 3c.

	Control TiO_2	**La-TiO_2**	**Li-TiO_2**
Films	3.08	3.07	2.92
Powders	3.06	3.07	2.92

Table S3. Photovoltaic characteristics of DSSCs made in this study using control, Li-TiO_2 or La-TiO_2 light-scattering layers of the photoanodes. Median values and standard deviations displayed in this table were calculated based on measurements from 5 identical devices.

	J_{SC} (mA cm^{-2})	**V_{OC} (mV)**	**FF (%)**	**PCE (%)**
Control TiO_2	12.8 (± 0.3)	738.1 (± 3.3)	56.2 (± 1.0)	5.3 (± 0.07)
Li- TiO_2	12.4 (± 0.2)	749.4 (± 4.8)	61.3 (± 1.5)	5.6 (± 0.2)
La- TiO_2	13.8 (± 0.2)	739.4 (± 2.8)	60.4 (± 1.3)	6.3 (± 0.2)

Table S4. The amount of adsorbed dye for control, La-TiO_2 and Li-TiO_2 NFs. The dye uptake measurements were performed on 1 x 1.5 cm large films that consisted of only one TiO_2 nanofiber layer.

Sample	Dye uptake (µg)
Control TiO_2	53.9
La- TiO_2	66.6
Li- TiO_2	55.7

Table S5. Average shunt (R_{SH}) and series resistance (R_S) measurements for every type of a DSSC device, extracted from the JV measurements.

Device	R_{SH} (Ω cm^{-2})	R_S (Ω cm^{-2})
Control TiO_2	1147	16.8
Li- TiO_2	3387	13.4
La- TiO_2	2351	16.5

The lowest series resistance (R_S) were obtained for La-TiO_2 NF devices. Typically, lowering the R_S results in an increase in FF. Compared to the control, both, namely La-TiO_2 and Li-TiO_2 NF devices exhibited lower R_S which supports the trends in Table S3 and S5. It is well known for other applications that the La modification of TiO_2 can have catalytic properties.[1] Therefore, the lowering of the R_S may indicate that the metal salt modification is effective at catalysing the oxidation of the I^- at the photoanode to regenerate the dye molecules. Trends in FF are also consistent with the results of the shunt resistance (R_{SH}) where both TiO_2 modified devices had higher R_{SH} as opposed to control with the lowest values (Table S5). Low R_{SH} are associated with power losses in a device as a result of an alternative current path for the light-generated current. Therefore, high R_{SH} is desirable since it indicates low current leakage in a device and it should ideally approach infinity. If the value is larger than 6 x 10^3 Ω cm^2, the influence of R_{SH} on FF can be neglected.[2] As our results show (Table S5), current leakage was present in all our devices, however it was the highest for the control DSSCs which resulted in their lowest FF (Table S3).

Table S6. Photovoltaic characteristics of PSC made in this study using either control, Li-TiO_2 or La-TiO_2 mesoporous layers for the photoanodes. Median values and standard deviations displayed in this table were calculated based on measurements from 5 identical devices.

	J_{SC} (mA cm^{-2})	V_{OC} (mV)	FF (%)	PCE (%)
Control TiO_2	19.8 (± 0.2)	801.1 (± 24.6)	54.6 (± 3.85)	8.8 (± 0.5)
Li- TiO_2	17.4 (± 0.6)	842.7 (± 15.0)	50.8 (± 2.7)	7.5 (± 0.7)
La- TiO_2	21.6 (± 0.7)	850.8 (± 15.7)	62.0 (± 1.9)	11.4 (± 0.4)

Table S7. Average shunt (R_{SH}) and series resistance (R_S) measurements for every type of a PSC device, extracted from the JV measurements.

Device	R_{SH} (Ω cm^{-2})	R_S (Ω cm^{-2})
Control TiO_2	206	11.1
Li- TiO_2	289	15.7
La- TiO_2	1392	8.8

Comparing to the control, the R_S was lower for the La-TiO_2 devices while the R_{SH} exhibited higher values. (Table S7) Such trend supports the enhancement of FF (Table S6). The R_{SH} can be associated with the current leakage that is induced by the pinholes in the cell or the current leakage from the edge of the device.[2] Since the value was not higher than 6000 Ω cm^2 the current leakage was present, however it was reduced upon the La modifications which resulted in a better photovoltaic performance. On the other hand, Li-TiO_2 devices exhibited the highest R_S while R_{SH} was higher than control but lower comparing to La-TiO_2 devices. Despite the trends in R_{SH} we believe that the main reason for the lower FF of Li-TiO_2 devices was a result of high R_S.

[1] I. Ivanova, T. A. Kandiel, Y.-J. Cho, W. Choi, D. Bahnemann, *ACS Catal.* **2018**, *8*, 2313–2325.
[2] B. Qi, J. Wang, *Phys. Chem. Chem. Phys.* **2013**, *15*, 8972–8982.